Finite Element Time Domain Method Using Piecewise Constant Basis Functions

Wilson A. Artuzi Jr., Member, IEEE

Abstract— **Whitney differential forms used in finite elemente time domain methods for electrodynamic computations are replaced by simpler piecewise constant forms in order to arrive at a concise, explicit and stable time domain formulation to be used with unstructured grids. As a result, a simple computational algorithm has been implemented and numerical tests demonstrate its advantages over some finite difference time domain approaches.**

Keywords— **FETD, FDTD, Differential Forms, Yee Cell**

I. Introduction

Time domain numerical solutions of Maxwell's equations have become powerful tools to predict and analyze innumerous devices and phenomena involving electromagnetic wave propagation. Among them there are two approaches of great importance: the finite difference time domain (FDTD) and the finite element time domain (FETD) methods [1], [2].

The FDTD method, which is based on separate staggered orthogonal grids for the electric and magnetic field discretizations in space, has provided a robust second-order accurate algorithm for time domain electrodynamic computations and its use has been widely spread despite of the fact that arbitrary shaped structures do not match the orthogonal lattice. Several approaches have been deviced in order to overcome this drawback. Some of them maintain the orthogonal grid basis [3] while others are implemented on unstructured grids [4]–[6].

On the other hand, the FETD method is conventionally applied to unstructured grids which are conformal to non-rectangular shapes. Significant improvements on FETD techniques have been achieved with the rediscovery of Whitney differential forms [7]. Unfortunately, they are well suited for tetrahedral grids only and yield implicit schemes in general [8].

The objective of this work is to replace Whitney forms in FETD by simpler piecewise constant forms and arrive at a concise, explicit and stable time domain formulation for unstructured grids. Accuracy issues are addressed through the evaluation of the resonant frequency of a metallic cylindrical cavity under different mesh conceptions.

II. Geometric Definitions

The mathematical treatment of the problem will be focused on elementary grids at first and the formulation for the whole problem will be achieved later by superposition. The combination of staggered elementary primal and dual grids comprising a region of homogeneous medium will be called a cell.

For simplicity, the following explanation will be based on a tetrahedral cell, as shown in Fig.1, though it can be extended to any other convex polyhedral cell. The primal

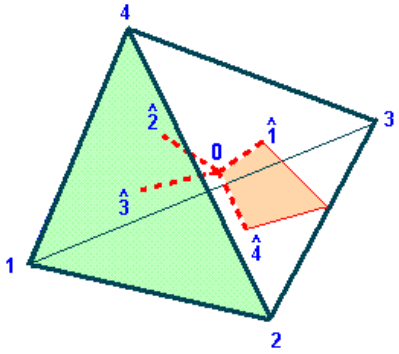

Fig. 1. A tetrahedral cell. Points 1, 2, 3 and 4 are referred to the primal grid (solid lines) and points 0, $\hat{1}$, $\hat{2}$, $\hat{3}$ and $\hat{4}$ are referred to the dual grid (dotted lines). Highlighted surfaces indicate the primal face 3 and the dual face 23.

grid is formed by points 1, 2, 3 and 4 which are provided as the output of mesh generators. Connection of two points by a straight line form a primal edge to be denoted by two indices in reference to these points. Three of these edges form a primal face to be denoted by one index in reference to the point excluded from this face. The dual grid consists of a point 0 inside the cell and one point on each face $\hat{1}$, $\hat{2}$, $\hat{3}$ and $\hat{4}$. Up to this point, there is no rule adopted to find the specific locations of these points. Connection of point 0 with a point on a face by a straight line form a dual edge whose index indicates the correspondence with this point. Two of these edges define a dual face whose indices correspond to the points excluded from this face.

III. Discrete Wave Equation

Using the notation of differential forms [9], Maxwell's curl equations are expressed as

$$\frac{\partial}{\partial t}B = -dE \quad (1)$$

$$\frac{\partial}{\partial t}D = dH \quad (2)$$

where E and H are the 1-form electric and magnetic field intensities, D and B are the 2-form electric and magnetic flux densities, respectively, and d is the exterior derivative

W. A. Artuzi Jr. is with Department of Electrical Engineering, Parana Federal University, Curitiba , PR, Brasil, artuzi@eletrica.ufpr.br.

which plays the roll of a curl operator when applied to 1-forms [9]. The equations above can be discretized over one cell and represented by matrix equations through integration of 1-forms along edges and 2-forms over faces in order to obtain

$$\frac{\partial}{\partial t}[B_p] = -[d_{p,ij}][E_{ij}] \quad (3)$$

$$\frac{\partial}{\partial t}[D_{kl}] = [d_{kl,q}][H_q] \quad (4)$$

where

$$B_p = \int_p B \quad \text{and} \quad E_{ij} = \int_{ij} E \quad (5)$$

are scalars that represent the magnetic flux through the primal face p and the electric potential difference along the primal edge ij,

$$D_{kl} = \int_{kl} D \quad \text{and} \quad H_q = \int_q H \quad (6)$$

are scalars that represent the electric flux through the dual face kl and the magnetic potential difference along the dual edge q, respectively, $[d_{p,ij}]$ and $[d_{kl,q}]$ are the primal and dual discrete exterior derivative operators (incidence matrices) which perform the summation of quantities assigned to the edges of a face, respecting their global orientations. The primal and dual operators are the transpose of each other ($[d_{kl,q}] = [d_{p,ij}]^T$).

Equations (3) and (4) are purely topological and exact, i.e., they do not contain any metric nor constitutive information and no approximation has been made thus far.

IV. Piecewise Constant Approximation

Metric and constitutive information are contained in the relations

$$D = \varepsilon * E \quad \text{and} \quad H = \nu * B \quad (7)$$

where ε and ν are, respectively, the electric permittivity and the inverse of the magnetic permeability which characterize the homogeneous medium inside a cell and $*$ denotes the Hodge operator [9] which converts between 1- and 2-forms while preserving their orthogonality. In order to reach the discrete forms of the constitutive relations it is necessary to introduce some approximations. In FETD methods, B and E inside a cell are usually expanded into sets of Whitney forms. The first order Whitney forms can be thought of as piecewise linear basis functions for tetrahedral cells [2]. In this work, these will be substituted by piecewise constant basis functions. For electric quantities, the tetrahedral cell is subdivided into 6 subsections , each one containing a primal edge and a dual face to be denoted by V_{ij}, as depicted in Fig.2(a), and for magnetic quantities, it is subdivided into 4 subsections, each one containing a primal face and a dual edge to be denoted by V_p, as shown in Fig.2(b). These give

$$B = \sum_p B_p W_p \quad , \quad W_p = \begin{cases} dS_p/S_p & \text{within } V_p \\ 0 & \text{elsewhere} \end{cases} \quad (8)$$

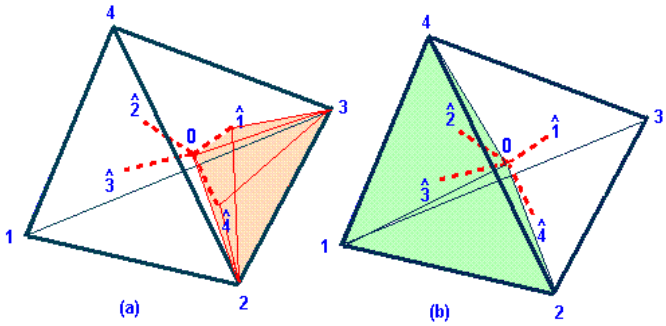

Fig. 2. Cell subdivisions for (a) electric and (b) magnetic quantities. Highlighted regions indicate (a) V_{23} and (b) V_3.

and

$$E = \sum_{ij} E_{ij} W_{ij} \quad , \quad W_{ij} = \begin{cases} dL_{ij}/L_{ij} & \text{within } V_{ij} \\ 0 & \text{elsewhere} \end{cases} \quad (9)$$

where dS_p and S_p are the differential and total areas of the primal face p and dL_{ij} and L_{ij} are the differential and total lengths of the primal edge ij. The constitutive relations are then used to find

$$D = \sum_{ij} E_{ij}\ \varepsilon * W_{ij}\ ,\ * W_{ij} = \begin{cases} *dL_{ij}/L_{ij} & \text{within } V_{ij} \\ 0 & \text{elsewhere} \end{cases} \quad (10)$$

and

$$H = \sum_p B_p\ \nu * W_p\ ,\ * W_p = \begin{cases} *dS_p/S_p & \text{within } V_p \\ 0 & \text{elsewhere} \end{cases} \quad (11)$$

where $*dL_{ij}$ is a differential area orthogonal to dL_{ij} and $*dS_p$ is a differential length orthogonal to dS_p. The application of integrals (5) and (6) conducts to the desired relations. If a barycentric subdivision is adopted with 0 being the barycenter of the cell and $\hat{1}$, $\hat{2}$, $\hat{3}$ and $\hat{4}$ being the barycenter of each primal face, the volume V of the cell is equally subdivided and the result is

$$[D_{kl}] = [\varepsilon_{kl,ij}][E_{ij}] \quad \text{and} \quad [H_q] = [\nu_{q,p}][B_p] \quad (12)$$

with

$$\varepsilon_{kl,ij} = \delta_{kl,ij}\ \frac{3V\varepsilon}{N_e\ L_{ij}^2} \quad \text{and} \quad \nu_{q,p} = \delta_{q,p}\ \frac{3V\nu}{N_f\ S_p^2} \quad (13)$$

being $\delta_{kl,ij}$ and $\delta_{q,p}$ Kronecker deltas, N_e and N_f, the number of edges and faces of the cell, respectively. Finally, (3), (4) and (12) can be combined to give the second-order wave equation

$$\frac{\partial^2}{\partial t^2}[\varepsilon_{kl,ij}][E_{ij}] = -[d_{kl,q}][\nu_{q,p}][d_{p,ij}][E_{ij}] \quad (14)$$

to be converted into a global equation by performing the superposition of cells when the edges are globally addressed. The time stepping solution is attained through the conventional central difference approximation of the time derivative.

The inspection of (13) sheds light onto the following aspects:

- the dual grid is virtual, i.e., the coordinates of points 0, $\hat{1}$, $\hat{2}$, $\hat{3}$ and $\hat{4}$ are not needed,
- $[\varepsilon_{kl,ij}]$ is a diagonal matrix, therefore the inversion of its global counterpart is straightforward and an explicit algorithm can be implemented,
- $V\varepsilon$ and $V\nu$ characterize the weighted volume averaging of ε and ν among cells of different media which share a common edge or face, respectively,
- $3V/N_eL_{ij}$ and $3V/N_fS_p$ are the area and the length of the orthogonal projection of the dual grid elements with respect to their primal counterparts as a consequence of the Hodge operator in the constitutive relations,
- the expressions are valid for any convex polyhedral cell if the barycentric subdivision criterion is maintained,
- the use of orthogonal hexahedral cells is equivalent to the implementation of the conventional FDTD method.

The barycentric subdivision in conjunction with the proposed basis functions ensure both a perfect rendering for the whole domain, thus charge conservation laws are implicit in the formulation since flux leakages are avoided. The electric conductivity σ can be included by adding the term $\frac{\partial}{\partial t}[\sigma_{kl,ij}][E_{ij}]$ in the left-hand side of (14), being $[\sigma_{kl,ij}]$ calculated as $[\varepsilon_{kl,ij}]$ with ε replaced by σ. Moreover, the algorithm is second-order accurate only if the cells are composed of regular polyhedra, otherwise, it presents local first-order truncation errors [10].

V. Numerical Experiments

Testing of the proposed formulation is implemented by computing the resonant frequency of a metallic cylindrical cavity under different mesh conceptions. The cavity is filled with air and it has a diameter of 380mm and a height of 300mm.

A. Modeling

The perfect electric conductor boundaries are obtained by imposing null electric fields on them. An electric field hard source is impressed on a longitudinal line across the cylindrical surface in order to excite the fundamental TM_{010} mode. The source shape in time is a Gaussian pulse having a width of 2.5ns to span significant field amplitudes up to the resonant frequency. Electric field samples are taken along the cavity axis during 50ns and are Fourier transformed to identify the resonant frequency value.

Two types of meshes are utilized: unstructured tetrahedral, as shown in Fig.3(a), and non-orthogonal structured hexahedral, as shown in Fig.3(b).

B. Convergence and Accuracy

The average length of the edges are varied in order to verify convergence and accuracy aspects of the proposed method. As shown in Fig.4, the relative errors of the resonant frequency are taken against the average number of divisions in space with respect to the free space wavelength at the theoretical resonant frequency value.

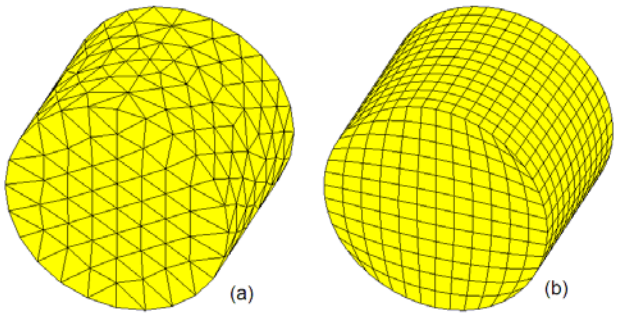

Fig. 3. Meshes for the space discretization of the cylindrical cavity: (a) unstructured tetrahedral and (b) non-orthogonal structured hexahedral.

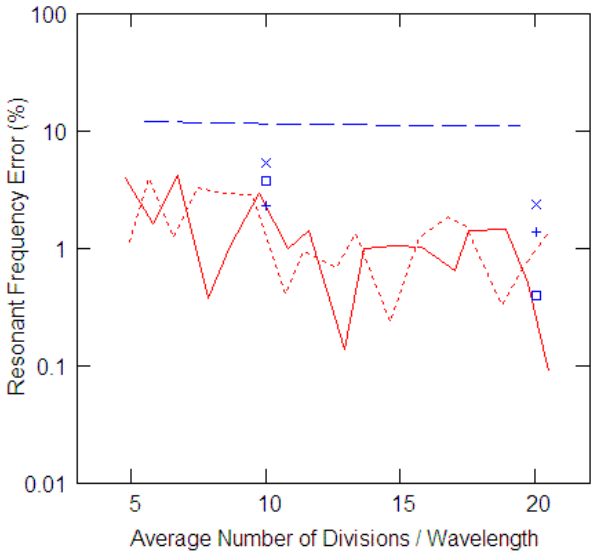

Fig. 4. Percentual error of the resonant frequency against the average number of divisions per free space wavelength for tetrahedral meshes (— whole cylinder, ··· one quarter of cylinder) and hexahedral meshes (- - this method, × staircasing, + contour-path, □ Dey-Mittra).

The solid and dotted lines represent the errors obtained with tetrahedral meshes. The solid line corresponds to the discretization of the whole cylinder while the dotted line corresponds to the discretization of one quarter of the structure which must give similar results because the field distributions of the mode are symmetric with respect to the cavity axis. It can be observed that the errors have a decreasing behavior when the number of divisions is increased, as it is expected. The curves are not smooth due to the randomness inherent to the tetrahedral mesh generation. The dashed line represents the errors obtained with non-orthogonal hexahedral meshes. Conversely, the curve is smooth because the mesh keeps the same pattern while being refined. The magnitude of the error, however, does not decrease as desired. For comparison, results ob-

tained with orthogonal grid FDTD simulations are plotted together [3]. In these simulations, the cavity is tilted with respect to the grid axes and the maximum error is taken. The staircasing approach (cross marks) leads to the highest errors, the contour-path approach (plus marks) presents errors similar to those obtained with the tetrahedral meshes and the Dey-Mittra approach (square marks) reaches better results for refined meshes.

C. Stability

It has been verified from the numerical results that an appropriate criterion for the maximum allowable time step can be set up as

$$\Delta t_{\max} = \frac{2R_{\min}}{\sqrt{3}\ c} \tag{15}$$

where $R_{\min}$ is the smallest cell inradius and c is the speed of light in vacuum. Formula (15) is compatible with the stability criterion for the FDTD method using cubic grids [1]. Under this condition, the method presented stability for long term simulations as large as 50.000 iterations, independent on the mesh being used.

D. Discussion

The comparison of the results shows immediately that the present method is not suitable for non-orthogonal hexahedral meshes. This fact can be explained by the local first-order truncation error caused by the piecewise constant approximation of the fields. The truncation error is maintained in the global equation because the mesh has a well defined pattern which is not altered when refined. On the other hand, the tetrahedral mesh, which uses the same kind of field approximation, does not propagate the first-order error to the global equation which surprisingly presents a second-order error behavior. This phenomenon is known as supra-convergence and is a consequence of the random nature of the mesh. The supra-convergence has been identified as a common property of random meshes and it has a mathematical prof in the case of rectangular meshes [10].

In terms of computational effort, it has been verified that the tetrahedral meshes have some disvantages in comparison with their hexahedral counterparts. The maximum allowable time step is about one half smaller and the number of unknowns is roughly triplicated for meshes with the same average length of edges, thus the total CPU time required for the simulation becomes six times larger. Nevertheless, the accuracy is better than the staircasing approach and comparable to the contour-path technique.

As a final remark, it should be stated that general purpose tetrahedral mesh generation tools can be easily incorporated by the presented technique while the other FDTD approaches mentioned here require custom algorithms for their mesh implementations.

VI. Conclusion

A concise, explicit and stable time domain formulation for electrodynamic computations using unstructured grids has been presented. The method is simple in implementation and the results have shown that although it has a local first-order truncation error, it becomes globally second-order accurate when using unstructured tetrahedral meshes. Accuracy is better than the conventional staircasing approach commonly used in FDTD methods and it is comparable to the contour-path approach which is a refined FDTD technique for arbitrary shaped structures.

This paper presents the first results obtained by this technique, but it appears as a promising approach to be used together with usual FETD techniques in order to reach a better compromise between computational effort and accuracy.

References

[1] A. Taflove, *Computational Electrodynamics: The Finite-Difference Time-Domain Method*, Artech House, Boston, 1995.

[2] J. F. Lee, "WETD — A finite element time domain approach for solving Maxwell's equations," *IEEE Microwave and Guided Wave Letters*, vol.4, pp.11-13, Jan. 1994.

[3] C. J. Railton and J. B. Schneider, "An analytical and numerical analysis of several locally conformal FDTD schemes," *IEEE Transactions on Microwave Theory and Tech.*, vol.47, pp.56-66, Jan. 1999.

[4] N. K. Madsen, "Divergence preserving discrete surface integral methods for Maxwell's curl equations using non-orthoonal unstructured grids, " *Journal of Computational Physics*, vol.119, pp.34-45, 1995.

[5] S. D. Gedney, F. S. Lansing and D. L. Rascoe, "Full wave analysis of microwave monolithic circuit devices using a generalized yee-algorithm based on unstructured grid, " *IEEE Trans. Microwave Theory and Tech.*, vol.44, pp.1393-1400, Aug. 1996.

[6] H. Sangani, J. T. Elson and C. H. Chan, "An explicit time-domain method using three-dimensional Whitney elements, " *Microwave and Opt. Technol. Lett.*, vol.7, no.13, pp.607-609, 1994.

[7] A. Bossavit, "Whitney forms: a class of finite elements for three-dimensional computations in electromagnetism," *IEE Proceedings*, vol.135, pt.A, pp.493-500, Nov. 1988.

[8] S. D. Gedney and U. Navsariwala, "An unconditionally stable finite element time-domain solution of the vector wave equation, " *IEEE Microwave and Guided Wave Lett.*, vol.5, pp.332-334, Oct. 1995.

[9] K. F. Warnick, R. H. Selfridge and D. V. Arnold, "Teaching electromagnetic field theory using differential forms," *IEEE Transactions on Education*, vol.40, pp.53-68, Feb. 1997.

[10] P. Monk and E. Suli, "Error estimates for Yee's method on non-uniform grids," *IEEE Transactions on Magnetics*, vol.30, pp.3200-3202, Sep. 1994.